

1 **Anthropogenic control over wintertime oxidation of atmospheric  
2 pollutants**

3  
4 J.D. Haskins,<sup>1</sup> F.D. Lopez-Hilfiker,<sup>1†</sup> B. H. Lee,<sup>1</sup> V. Shaw,<sup>1††</sup> G. M. Wolfe,<sup>2,3</sup> J. DiGangi,<sup>4</sup> D.  
5 Fibiger,<sup>5,13</sup> <sup>†††</sup>E.E. McDuffie,<sup>5,6,13</sup> <sup>‡</sup>P. Veres,<sup>5</sup> J.C. Schroder,<sup>5,6</sup> P. Campuzano-Jost,<sup>5,6</sup> D.A. Day,<sup>5,6</sup>  
6 J. Jimenez,<sup>5,6</sup> A. Weinheimer,<sup>7</sup> T. Sparks,<sup>8</sup> C. Ebben,<sup>8</sup> R. C. Cohen,<sup>8</sup> T. Campos,<sup>7</sup> A. Sullivan,<sup>9</sup> H.  
7 Guo,<sup>10</sup> R. Weber,<sup>10</sup> J. Dibb,<sup>11</sup> J. Greene,<sup>12</sup> M. Fiddler,<sup>12</sup> S. Bililign,<sup>12</sup> L. Jaegle,<sup>1</sup> S.S. Brown,<sup>7,13</sup>  
8 J.A. Thornton<sup>1\*</sup>

9  
10 <sup>1</sup> Department of Atmospheric Sciences, University of Washington, Seattle, WA USA

11 <sup>2</sup> Joint Center for Earth Systems Technology, University of Maryland Baltimore County,  
12 Baltimore, MD USA

13 <sup>3</sup>Atmospheric Chemistry and Dynamics Laboratory, NASA Goddard Space Flight Center,  
14 Greenbelt, MD USA

15 <sup>4</sup>NASA Langley Research Center, Hampton, VA USA

16 <sup>5</sup> Cooperative Institute for Research in Environmental Sciences, University of Colorado, Boulder,  
17 CO, USA

18 <sup>6</sup> Department of Chemistry, University of Colorado, Boulder, CO USA

19 <sup>7</sup> Earth Observing Laboratory, National Center for Atmospheric Research, Boulder, CO USA

20 <sup>8</sup> Department of Chemistry, University of California, Berkeley CA USA

21 <sup>9</sup> Department of Atmospheric Sciences, Colorado State University, Fort Collins, CO USA

22 <sup>10</sup> School of Earth and Atmospheric Sciences, Georgia Institute of Technology, Atlanta, GA USA

23 <sup>11</sup> Department of Earth Sciences, University of New Hampshire, Durham, NH USA

24 <sup>12</sup> Department of Physics, North Carolina A&T State University, Greensboro, NC USA

25 <sup>13</sup> Chemical Sciences Division, NOAA Earth System Research Laboratory, Boulder, CO USA

26  
27 <sup>†</sup> Now at Tofwerk AG, Switzerland

28 <sup>††</sup> Now at Harvard University, Cambridge, USA

29 <sup>†††</sup> Now at California Air Resources Board, Sacramento, USA

30 <sup>‡</sup> Now at the Department of Physics and Atmospheric Science, Dalhousie University, Halifax,  
31 NS, Canada

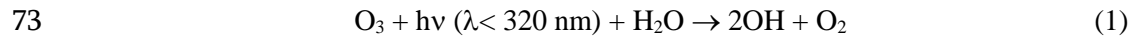
32  
33 <sup>\*</sup> Correspondence to: [thornton@atmos.washington.edu](mailto:thornton@atmos.washington.edu)

50 Anthropogenic air pollutants such as nitrogen oxides ( $\text{NO}_x = \text{NO} + \text{NO}_2$ ), sulfur dioxide ( $\text{SO}_2$ ),  
51 and volatile organic compounds (VOC), among others, are emitted to the atmosphere  
52 throughout the year from energy production and use, transportation, and agriculture. These  
53 primary pollutants lead to the formation of secondary pollutants such as fine particulate  
54 matter ( $\text{PM}_{2.5}$ ) and ozone ( $\text{O}_3$ ) [Seinfeld, 1989; Dabdub et al., 1997; Jacobson et al., 2000;  
55 Volkamer et al., 2006;], as well as to acid and nutrient deposition to ecosystems [Schofield,  
56 1976; Irwin et al., 1988; Menz et al., 2004; Greaver et al., 2012;] and perturbations to the  
57 abundance and lifetimes of short-lived greenhouse gases [Wang et al., 1976; Fishman et al.,  
58 1980; Jacob & Winner, 2009; Ramanathan et al., 2009;]. Free radical oxidation reactions  
59 driven by solar radiation govern the atmospheric lifetimes and transformations of most  
60 primary pollutants and thus their spatial distributions [Weinstock, 1969; Levy, 1971; Seinfeld,  
61 1989; Collins et al., 2002;]. During winter in the mid and high latitudes, where a large fraction  
62 of atmospheric pollutants are emitted globally, such photochemical oxidation is significantly  
63 slower [Levy et al., 1985; Klonecki & Levy, 1997; Yienger et al., 1999]. Using observations  
64 from a highly instrumented aircraft, we show that multi-phase reactions between gas-phase  
65  $\text{NO}_x$  reservoirs and aerosol particles, as well as VOC emissions from anthropogenic activities,  
66 lead to a suite of atypical radical precursors dominating the oxidizing capacity in polluted  
67 winter air, and thus, the distribution and fate of primary pollutants on a regional to global  
68 scale.

69

70 In the warmer and more photochemically active summer months, the photolysis of ozone ( $\text{O}_3$ ) in  
71 the presence of water vapor leads to production of hydroxyl radicals ( $\text{OH}$ ).

72



73

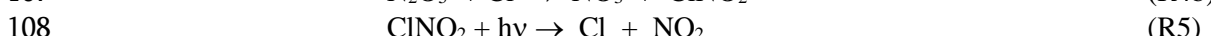
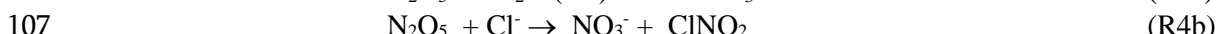
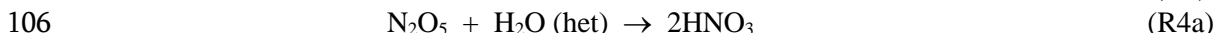
74 OH radicals initiate the rapid formation of multiple secondary pollutants such as  $\text{O}_3$  and secondary  
75 organic aerosols (SOA) during volatile organic compound (VOC) degradation, as well as sulfuric  
76 acid and nitric acid ( $\text{HNO}_3$ ) from reaction with sulfur dioxide and nitrogen dioxide ( $\text{NO}_2$ ). During  
77 winter, primary radical production via R1 is reduced by more than an order of magnitude due to  
78 the combination of reduced sunlight and water vapor [Klonecki & Levy, 1997; Yienger et al., 1999].  
79 Therefore, pollutants, such as nitrogen oxides ( $\text{NO}_x = \text{NO} + \text{NO}_2$ ), VOC, and  $\text{SO}_2$ , oxidize more  
80 slowly during winter and spread over wider geographic areas than during summer. The overall  
81 lower radical production expected during winter suggests a higher sensitivity to the presence of less  
82 common radical sources. Yet, few observational constraints of wintertime radical precursors exist  
83 on scales suitable to test models of pollutant transport and transformations.

84

85 During winter, multiphase processes and direct emissions of photo-labile molecules significantly  
86 influence the primary radical budget. For example, at night, nitrogen dioxide ( $\text{NO}_2$ ) reacts with  $\text{O}_3$   
87 to generate the nitrate radical ( $\text{NO}_3$ ), which subsequently reacts with  $\text{NO}_2$  to form dinitrogen  
88 pentoxide ( $\text{N}_2\text{O}_5$ ). In winter,  $\text{N}_2\text{O}_5$  is a major nocturnal reservoir of  $\text{NO}_x$  radicals and known to  
89 react on aerosol particles, clouds, and ground surfaces, but not in the gas-phase. Aerosol particles  
90 often have significant liquid water, catalyzing the hydrolysis of  $\text{N}_2\text{O}_5$  to two  $\text{HNO}_3$  molecules,  
91 thereby limiting the lifetime of  $\text{NO}_x$  and impacting  $\text{PM}_{2.5}$  and acid deposition through subsequent  
92 gas-particle partitioning of  $\text{HNO}_3$  to form particulate nitrate ( $\text{pNO}_3^-$ ) or deposition of  $\text{HNO}_3$  to the  
93 ground [Platt and Heintz, 1994; Richards, 1983; Dentener and Crutzen, 1993; Smith et al., 1995;  
94 Alexander et al., 2009;]. In particles with sufficient chloride content ( $\text{pCl}^-$ ),  $\text{N}_2\text{O}_5$  will react  
95 predominantly to form nitryl chloride and  $\text{pNO}_3^-$  [Finlayson-Pitts et al., 1989; Behnke & Zetzsch,  
96 1990; Zetzsch & Behnke, 1992]. During the morning hours,  $\text{ClNO}_2$  undergoes photolysis  
97 recycling  $\text{NO}_x$ , increasing its lifetime and transport from source regions, while also releasing  
98 highly reactive chlorine radicals ( $\text{Cl}$ ), which initiate the oxidation of hydrocarbons as fast or even  
99 10 to 100 times faster than  $\text{OH}$  [Orlando et al., 2003; Platt & Hönniger, 2003; Simpson et al.,

101 2015].  $\text{N}_2\text{O}_5$  that does not react overnight quickly becomes  $\text{NO}_x$  during the subsequent day due to  
102  $\text{NO}_3$  radical photochemistry.

103



110

111 Utilizing the NSF/NCAR C-130 aircraft during the WINTER campaign, simultaneous airborne  
112 observations of all components involved in the conversion of  $\text{NO}_x$  to  $\text{N}_2\text{O}_5$  and its corresponding  
113 multiphase reactants and products were made (See Figure 1 and supplemental information, SI).  
114 Mixing ratios of speciated nitrogen oxides measured by mass spectrometry including  $\text{ClNO}_2$ ,  
115  $\text{N}_2\text{O}_5$ ,  $\text{HNO}_3$ , and nitrous acid (HONO), together with NO and  $\text{NO}_2$  measured by  
116 chemiluminescence (Figure 1, top panels) explain the independently measured sum total reactive  
117 nitrogen abundance ( $\text{NO}_y = \text{NO}_x + 2^* \text{N}_2\text{O}_5 + \text{ClNO}_2 + \text{HNO}_3 + \text{HONO} + \dots$ ) at all points along the  
118 flight track (Figure 1, bottom). Westerly winds export  $\text{NO}_x$  emissions from the polluted urban  
119 corridor of the Northeast U.S. into the marine boundary layer (MBL) over the Atlantic Ocean.  
120 Over the course of a winter night, our observations show that ~25-50% of  $\text{NO}_x$  is converted to  
121  $\text{N}_2\text{O}_5$ , much of which reacts in the MBL to form  $\text{HNO}_3$  and  $\text{ClNO}_2$  (see SI).

122

123 Using the suite of *in situ* observations, we can directly assess the importance of each radical  
124 source to the oxidative capacity of the wintertime atmosphere (See SI for details). An example set  
125 of results from such calculations is shown in Figure 1 (c). We use observed nighttime  
126 concentrations of  $\text{O}_3$ , humidity,  $\text{ClNO}_2$ , formaldehyde (HCHO), and HONO together with  
127 modeled photolysis frequencies to calculate the total integrated concentration of radicals that  
128 would be produced by these precursors over the following day. Other radical sources, such as  
129 from alkene ozonolysis or dihalogen photolysis were small on a regional basis during WINTER  
130 (see SI). While the nocturnal atmosphere near the surface over land is poorly mixed (See SI),  
131 vertical profiling provided by the aircraft allowed us to uniquely assess the vertical extent of these  
132 radical precursors. As expected, we found that over relatively warmer water in the MBL, air is  
133 relatively well mixed up to 800-1500 m altitude (e.g. Figure 2), allowing more straightforward  
134 calculations of radical budgets from measured concentrations.

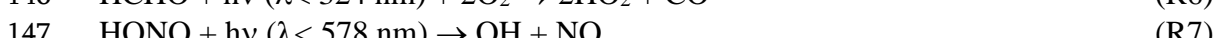
135

136 As pollution is transported offshore overnight, and  $\text{ClNO}_2$  formation continues, we find that  
137  $\text{ClNO}_2$  photolysis (R5) becomes the single largest source of radical oxidants. The latest pollution  
138 intercept occurred before midnight local time, and several more hours of  $\text{N}_2\text{O}_5$  production and  
139 multiphase chemistry could be expected. Estimates of  $\text{N}_2\text{O}_5$  reactivity on aerosol particles and  
140  $\text{ClNO}_2$  yield derived from *in situ* observations [McDuffie et al., 2018a; McDuffie et al., 2018b;] suggest  
141  $\text{ClNO}_2$  concentrations would have continued to increase overnight, accounting for as  
142 much as 80% of the daytime radical source the next day.

143

144 Other important observed radical sources are  $\text{O}_3$  via R1, HCHO via R6 and HONO via R7.

145



148

149 HCHO photolysis leads to the net formation of two HO<sub>2</sub> radicals, which rapidly cycle to OH in  
150 the presence of NO. Annual HCHO sources are dominated by *in situ* VOC oxidation, but during  
151 winter, negligible biogenic emissions of isoprene [Goldstein et al., 1998; Luecken et al., 2012;],  
152 and overall lower radical concentrations, reduce the secondary production of HCHO. HCHO is  
153 directly emitted from a variety of anthropogenic activities, e.g. inefficient combustion and  
154 manufacturing processes [Sigsby et al., 1987; Altshuller, 1993; Anderson et al., 1996; Kelly et al.,  
155 1999], but with currently uncertain magnitudes and spatial distributions. The GEOS-Chem global  
156 transport model underestimates the observed WINTER HCHO by a factor of 2 on average (see  
157 SI). Increasing the direct anthropogenic emission of HCHO in the model by a factor of 5 brings  
158 the model into good agreement with the observations, with approximately half the HCHO in the  
159 model arising from secondary oxidation of anthropogenic VOC and half from direct emissions.  
160 Increasing the emissions of anthropogenic VOC that react on an hour timescale to produce  
161 HCHO instead of direct emissions of HCHO would also be consistent with the observations,  
162 though appropriate observational constraints are lacking. There is strong evidence that emissions  
163 of HCHO and related oxygenated VOC from automobiles are significantly higher in the  
164 wintertime due to the inefficient combustion associated with cold engine starts [Anderson et al.,  
165 1994; Anderson et al., 1996; Li et al., 2010; Clairotte et al., 2013]. Moreover, the observed  
166 HCHO is strongly correlated with tracers of fossil fuel and wood combustion (See SI). While  
167 smaller than the summertime HCHO sources from biogenic VOC degradation [Fortems-Cheiney  
168 et al., 2012; Luecken et al., 2012; Wolfe et al., 2016;], the wintertime anthropogenic emissions of  
169 HCHO or its precursors that we infer are very important to the regional source of radicals.  
170

171 HONO is both directly emitted from combustion [Kirchstetter et al., 1996; Stutz et al., 2002;],  
172 and formed *in situ* from multiphase chemistry of NO<sub>2</sub> as well as pNO<sub>3</sub><sup>-</sup> photolysis [Kleffmann,  
173 2007; Zhou et al., 2011;]. Figure 1 shows that the measured nighttime HONO concentrations are  
174 a small contributor to the primary daytime radical source over the surveyed domain. HONO is  
175 more important near the urban areas, very close to the surface (<100 m), and more generally  
176 enhanced over land than in the MBL (see SI). Our observations suggest a smaller role for HONO  
177 on a regional basis in the daily integrated radical budget than might be inferred from ground-  
178 based observations due to the poorly mixed nocturnal atmosphere [Febo et al., 1996; Stutz et al.,  
179 2002; Wong et al., 2012]. However, the estimates in Figure 1 neglect a potential source from  
180 pNO<sub>3</sub><sup>-</sup> photolysis, which we assess below.  
181

182 The above estimates of daytime radical sources shown in Figure 1 evolve as expected at sunrise  
183 as shown in Figure 2. A stalled high-pressure system offshore of New Jersey allowed us a unique  
184 opportunity to make multiple transects throughout the morning (Figure 2a) of pollution from the  
185 greater New York City area that had aged overnight in the MBL (see SI). As the sun rose during  
186 the flight, vertical profiles (Figure 2b) conducted along various segments revealed that the  
187 instantaneous radical source from CINO<sub>2</sub> photolysis was 60-80% of the total primary radical  
188 source throughout the entire MBL. The importance of CINO<sub>2</sub> as a radical source decreased  
189 substantially at altitudes above the MBL, while that of O<sub>3</sub> via R1 increased as expected given the  
190 steep gradients in CINO<sub>2</sub> precursors (NO<sub>x</sub> and aerosol particles) between the polluted boundary  
191 layer and overlying free troposphere. The observed instantaneous production rate of radicals  
192 from CINO<sub>2</sub> was a factor of 5 to 10 larger than the other radical sources throughout the morning  
193 as the aircraft made multiple intercepts of the pollution plume. HONO photolysis was the next  
194 largest instantaneous radical source, in part due to its larger photolysis rate coefficient compared  
195 to HCHO. Nighttime N<sub>2</sub>O<sub>5</sub> chemistry is a removal mechanism for O<sub>3</sub> (R2-R4) [Platt et al., 1984;  
196 Brown et al., 2004] and as such O<sub>3</sub> mixing ratios are often suppressed in NO<sub>x</sub>-rich air masses  
197 during the night and morning [Stutz et al., 2004], which contributes in part to the negligible  
198 instantaneous source of radicals from R1 in the polluted MBL. The aircraft returned to its base  
199 (segment E, Figure 2A) by flying above the MBL, where we find that the background

200 tropospheric source of radicals is dominated by that from  $O_3$  photolysis (R1), consistent with  
201 expectations.

202  
203 We extend this instantaneous observational analysis during this flight using the Framework for 0-  
204 D Atmospheric Modeling (F0AM) (Wolfe et al., 2016) , which is based on the master chemical  
205 mechanism version 3.3.1 that explicitly tracks over 5800 chemical species in over 17,000  
206 reactions (Bloss et al., 2005; Jenkin et al., 1997, 2003; Saunders et al., 2003) by performing two  
207 simulations; one including and one excluding reactions from chlorine and heterogeneous  $N_2O_5$   
208 formation described in Riedel et al., (2014). Initializing F0AM with WINTER measurements of  
209 VOCs and inorganic gas phase species (see SI for details), Figure 3 shows the radical budget  
210 occurring the day following our interception of the maximum  $ClNO_2$  concentration observed,  
211 which occurred on this flight at 6:40am in Figure 2c at point D in Figure 2a. Consistent with our  
212 observational analysis, the F0AM predicted instantaneous radical production rate from  $ClNO_2$   
213 was a factor of 5 to 12 larger than the other largest radical source throughout the morning, shown  
214 in Figure 3. Excluding reactions involving chlorine in F0AM caused an underestimate in the  
215 integrated daily radical budget the following day of 1.8 ppbv, or a factor of 3.75. This  
216 underestimate occurs primarily from excluding the early morning source of Cl radicals from  
217  $ClNO_2$  photolysis, but also from a 114% enhancement (0.62 ppbv) in the integrated daily  
218 [HCHO] that occurred because of an increase in VOC oxidation by those Cl radicals (see SI), and  
219 an increase in the daily integrated ozone production of 4.7 ppbv, thereby increasing the local  
220 source of OH from  $O_3$  photolysis. These results highlight the importance of nocturnal  
221 heterogeneous chlorine chemistry in coupling the secondary oxidation of VOCs,  $NO_y$  and  $HO_x$   
222 cycling, in the overall predicted daily radical budget within the WINTER domain.  
223

224 We conducted 13 research flights, equally covering daytime and nighttime conditions, over land  
225 and the ocean, throughout the eastern U.S. domain (see Figure 1). Applying the above  
226 instantaneous radical source analysis to the wider set of flights illustrates the major importance of  
227 HCHO and  $ClNO_2$  as radical precursors, with both being more important in polluted air,  
228 represented by increasing  $NO_x$  mixing ratios as shown in Figure 4. These results illustrate the  
229 control of wintertime radical sources by anthropogenic emissions of  $NO_x$  and VOC, and  
230 subsequent multiphase chemistry, with > 70% of the radical source stemming not from the  
231 canonical reaction R1, but from  $ClNO_2$ , HCHO, and HONO photolysis. Daytime observations  
232 underestimate the overall contributions of HONO and  $ClNO_2$  to the total primary radical source  
233 because both species photolyze rapidly and may not be reformed until night. Over land, this effect  
234 causes an approximately 10% underestimate of the daily radical source from  $ClNO_2$ .  
235

236 More over, recent studies suggest photolysis of  $pNO_3^-$  may be an important daytime HONO  
237 source, which would not be captured by our strictly observational approach. If daytime  
238 production of HONO from  $pNO_3^-$  photolysis occurs at the seasonally adjusted rate recently  
239 suggested from summertime observations [Ye et al., 2016;], and which our observations do not  
240 contradict (see SI), then HONO photolysis integrated over the day would increase the total radical  
241 source shown in Figure 4 by ~50% over land, with smaller but non-negligible contributions in the  
242 polluted MBL (See SI). Thus, the primary radical budget during winter may well be larger, with  
243 even stronger connection to anthropogenic pollution and atypical radical sources than indicated  
244 by our conservative estimate shown in Figure 4.

245 HCHO emissions and the multiphase chemistry of nitrogen oxides that produces  $ClNO_2$ ,  $pNO_3^-$ ,  
246 and HONO, are highly parameterized components of air quality or chemistry climate models, if  
247 included at all [Behnke et al., 1997; Perice et al., 1998; Evans & Jacob et al., 2005; Riemer et al.,  
248 2003; Anttila et al., 2006; Guenther et al., 2006; Davis et al., 2008; Bertram & Thornton, 2009;  
249 Griffiths et al., 2009; Roberts et al., 2009; Vinken et al., 2011; Barkley et al., 2012; Ryder et al.,  
250

251 2015;]. Incorporating only  $\text{ClNO}_2$  and  $\text{HCHO}$  sources consistent with the observations from the  
252 WINTER campaign into the GEOS-Chem model of global atmospheric chemistry and transport,  
253 we find significant impacts on climate and air quality quantities. For example,  $\text{PM}_{2.5}$  components,  
254 such as SOA and sulfate increase, while nitrate decreases (see SI), and  $\text{NO}_x$  shifts further into its  
255 labile reservoirs, such as peroxy acetyl nitrate (PAN, see Figure 5). These changes are driven by  
256 subsequent increased concentrations of oxidant initiators such as  $\text{HO}_x$  ( $\text{OH} + \text{HO}_2$ ) radicals,  
257 which increase by 40-80% over the WINTER domain from increased  $\text{HCHO}$  photolysis and  $\text{VOC}$   
258 +  $\text{Cl}$  reactions, with concomitant increases in ozone production (see SI).

259

260 Wintertime sulfate is often underestimated by air quality models, while  $\text{pNO}_3^-$  and nitrate  
261 deposition over land have been overestimated [Tesche et al., 2002; Heald et al., 2012; Walker et  
262 al., 2012; Gao et al., 2016;]. Additionally, the split between primary and secondary OA remains  
263 poorly tested on a regional basis during winter [Fuzzi et al., 2006; Jimenez et al., 2009;]. The  
264 increases in regional radical oxidants and changes to  $\text{NO}_x$  multiphase chemistry implied by our  
265 observations reduce such discrepancies and uncertainties. Moreover, these changes halve model  
266 underestimates (from 30% to 15% bias) of total peroxy nitrates (such as PAN) measured during  
267 WINTER, providing additional support for increased oxidation initiated by atypical radical  
268 sources, and increased export of  $\text{NO}_x$  reservoirs to the global free troposphere.

269

270 We have shown that anthropogenic emissions of  $\text{NO}_x$  and of  $\text{HCHO}$  and its analogues exert  
271 control over the primary source of radical oxidants in polluted air during winter. In the case of  
272  $\text{HCHO}$ , the dormant wintertime biosphere strongly implies its wintertime sources are dominated  
273 by anthropogenic emissions, which are likely enhanced due to inefficient combustion, such as  
274 during vehicular cold-starts and residential wood smoke. In the case of  $\text{NO}_x$ , the natural shift  
275 towards nocturnal multi-phase processing and an availability of sea-spray derived particulate  
276 chloride allowed the first observational confirmation that its conversion to  $\text{ClNO}_2$  represents a  
277 critically important wintertime radical source throughout the polluted MBL that also serves to  
278 enhance  $[\text{HCHO}]$ . A daytime source of  $\text{HONO}$  from  $\text{pNO}_3^-$  photolysis, where the  $\text{pNO}_3^-$   
279 enhancements stem from multi-phase processing of  $\text{NO}_x$  emissions would only increase the  
280 importance of local and regional anthropogenic emissions over the wintertime radical budget.

281

282 The coupling of  $\text{NO}_x$  emissions, multiphase conversion to  $\text{pNO}_3^-$  and  $\text{ClNO}_2$ , and subsequent  
283  $\text{pNO}_3^-$  photolysis to  $\text{HONO}$  represent a potentially dominant source of radicals in polluted  
284 wintertime air. These insights lead to predictions of increased  $\text{PM}_{2.5}$  and increased export of  $\text{NO}_x$   
285 to the remote troposphere via PAN, where short-lived greenhouse gases such as  $\text{O}_3$  and  $\text{CH}_4$  are  
286 far more sensitive to its presence [Singh et al., 1981; Roberts et al., 1990]. Other regions of the  
287 world, such as China, Europe, and northern India also experience high  $\text{NO}_x$ , VOC sources from  
288 inefficient combustion and reactive chlorine during winter [Sarwar et al., 2014; Lowe et al., 2015;  
289 Li et al., 2016;]. Our findings therefore suggest important global scale revisions to our  
290 understanding of wintertime pollution transformations, transport and deposition.

291

292

293

294

295

296

297

298

299

300

301

302 **References**

303

304 Alexander, B., Hastings, M. G., Allman, D. J., Dachs, J., Thornton, J. A., & Kunasek, S. A.  
305 (2009). Quantifying atmospheric nitrate formation pathways based on a global model of the  
306 oxygen isotopic composition ( $\Delta^{17}\text{O}$ ) of atmospheric nitrate. *Atmos. Chem. Phys.*,  
307 9(14), 5043–5056. <https://doi.org/10.5194/acp-9-5043-2009>

308

309 Altshuller, A. P. (1993). Production of aldehydes as primary emissions and from secondary  
310 atmospheric reactions of alkenes and alkanes during the night and early morning hours.  
311 *Atmospheric Environment. Part A. General Topics*, 27(1), 21–32.  
312 [https://doi.org/https://doi.org/10.1016/0960-1686\(93\)90067-9](https://doi.org/https://doi.org/10.1016/0960-1686(93)90067-9)

313

314 Anderson, L. G., Lanning, J. A., Barrell, R., Miyagishima, J., Jones, R. H., & Wolfe, P. (1996).  
315 Sources and sinks of formaldehyde and acetaldehyde: An analysis of Denver's ambient  
316 concentration data. *Atmospheric Environment*, 30(12), 2113–2123.  
317 [https://doi.org/https://doi.org/10.1016/1352-2310\(95\)00175-1](https://doi.org/https://doi.org/10.1016/1352-2310(95)00175-1)

318

319 Anderson, L. G., Wolfe, P., Barrell, R. A., & Lanning, J. A. (1994). The effects of oxygenated  
320 fuels on the atmospheric concentrations of carbon monoxide and aldehydes in Colorado. In  
321 F. . Sterrett (Ed.), *Alternative Fuesl and the Environment* (pp. 75–103). Boca Raton,  
322 Florida: Lewis Publishers.

323

324 Anttila, T., Kiendler-Scharr, A., Tillmann, R., & Mentel, T. F. (2006). On the Reactive Uptake of  
325 Gaseous Compounds by Organic-Coated Aqueous Aerosols: Theoretical Analysis and  
326 Application to the Heterogeneous Hydrolysis of  $\text{N}_2\text{O}_5$ . *The Journal of Physical Chemistry A*,  
327 110(35), 10435–10443. <https://doi.org/10.1021/jp062403c>

328

329 Barkley, M. P., Kurosu, T. P., Chance, K., De Smedt, I., Van Roozendael, M., Arneth, A., ...  
330 Guenther, A. (2012). Assessing sources of uncertainty in formaldehyde air mass factors over  
331 tropical South America: Implications for top-down isoprene emission estimates. *Journal of  
332 Geophysical Research: Atmospheres*, 117(D13). <https://doi.org/10.1029/2011JD016827>

333

334 Behnke, W., & Zetzsch, C. (1990). Heterogeneous photochemical formation of Cl atoms from  
335 NaCl aerosol, NOx and ozone. *Journal of Aerosol Science*, 21, S229–S232.  
336 [https://doi.org/https://doi.org/10.1016/0021-8502\(90\)90226-N](https://doi.org/https://doi.org/10.1016/0021-8502(90)90226-N)

337

338 Behnke, W., George, C., Scheer, V., & Zetzsch, C. (1997). Production and decay of  $\text{ClNO}_2$  from  
339 the reaction of gaseous  $\text{N}_2\text{O}_5$  with NaCl solution: Bulk and aerosol experiments. *Journal of  
340 Geophysical Research: Atmospheres*, 102(D3), 3795–3804.  
341 <https://doi.org/10.1029/96JD03057>

342

343 Bertram, T. H., & Thornton, J. A. (2009). Toward a general parameterization of  $\text{N}_2\text{O}_5$  reactivity  
344 on aqueous particles: the competing effects of particle liquid water, nitrate and chloride.  
345 *Atmos. Chem. Phys.*, 9(21), 8351–8363. <https://doi.org/10.5194/acp-9-8351-2009>

346

347 Brown, S. S., Dibb, J. E., Stark, H., Aldener, M., Vozella, M., Whitlow, S., ... Ravishankara, A.  
348 R. (2004). Nighttime removal of NOx in the summer marine boundary layer. *Geophysical  
349 Research Letters*, 31(7). <https://doi.org/10.1029/2004GL019412>

350

351 Clairotte, M., Adam, T. W., Zardini, A. A., Manfredi, U., Martini, G., Krasenbrink, A., ...  
352 Astorga, C. (2013). Effects of low temperature on the cold start gaseous emissions from

353 light duty vehicles fuelled by ethanol-blended gasoline. *Applied Energy*, 102, 44–54.  
354 <https://doi.org/https://doi.org/10.1016/j.apenergy.2012.08.010>

355

356 Collins, W. J., Derwent, R. G., Johnson, C. E., & Stevenson, D. S. (2002). The Oxidation of  
357 Organic Compounds in the Troposphere and their Global Warming Potentials. *Climatic  
358 Change*, 52(4), 453–479. <https://doi.org/10.1023/A:1014221225434>

359

360 Committee on Aldehydes: National Research Council. (1981). *Formaldehyde and other  
361 aldehydes*. (N. Grossblatt, Ed.). Washington, D.C.: National Academy Press.

362

363 Dabdub, D., Meng, Z., & Seinfeld, J. H. (1997). Chemical bonding between atmospheric ozone  
364 and particulate matter. *Science*, 276, 116+. Retrieved from  
365 [http://link.galegroup.com/apps/doc/A19628485/AONE?u=wash\\_main&sid=AONE&xid=5eb5f24d](http://link.galegroup.com/apps/doc/A19628485/AONE?u=wash_main&sid=AONE&xid=5eb5f24d)

366

367

368 Davis, J. M., Bhave, P. V., & Foley, K. M. (2008). Parameterization of N<sub>2</sub>O<sub>5</sub> reaction probabilities  
369 on the surface of particles containing ammonium, sulfate, and nitrate. *Atmos. Chem. Phys.*,  
370 8(17), 5295–5311. <https://doi.org/10.5194/acp-8-5295-2008>

371

372 Dentener, F. J., & Crutzen, P. J. (1993). Reaction of N<sub>2</sub>O<sub>5</sub> on tropospheric aerosols: Impact on  
373 the global distributions of NO<sub>x</sub>, O<sub>3</sub>, and OH. *Journal of Geophysical Research: Atmospheres*, 98(D4), 7149–7163. <https://doi.org/10.1029/92JD02979>

374

375

376 Evans, M. J., & Jacob, D. J. (2005). Impact of new laboratory studies of N<sub>2</sub>O<sub>5</sub> hydrolysis on  
377 global model budgets of tropospheric nitrogen oxides, ozone, and OH. *Geophysical  
378 Research Letters*, 32(9). <https://doi.org/10.1029/2005GL022469>

379

380 Febo, A., Perrino, C., & Allegrini, I. (1996). Measurement of nitrous acid in milan, italy, by doas  
381 and diffusion denuders. *Atmospheric Environment*, 30(21), 3599–3609.  
382 [https://doi.org/https://doi.org/10.1016/1352-2310\(96\)00069-6](https://doi.org/https://doi.org/10.1016/1352-2310(96)00069-6)

383

384 Finlayson-Pitts, B. J., Ezell, M. J., & Pitts, J. N. (1989). Formation of chemically active chlorine  
385 compounds by reactions of atmospheric NaCl particles with gaseous N<sub>2</sub>O<sub>5</sub> and ClONO<sub>2</sub>.  
386 *Nature*, 337(6204), 241–244. <http://dx.doi.org/10.1038/337241a0>

387

388 Fishman, J., Ramanathan, V., Crutzen, P. J., & Liu, S. C. (1979). Tropospheric ozone and  
389 climate. *Nature*, 282(5741), 818–820. <https://doi.org/10.1038/282818a0>

390

391 Fortems-Cheiney, A., Chevallier, F., Pison, I., Bousquet, P., Saunois, M., Szopa, S., ... Fried, A.  
392 (2012). The formaldehyde budget as seen by a global-scale multi-constraint and multi-  
393 species inversion system. *Atmos. Chem. Phys.*, 12(15), 6699–6721.  
394 <https://doi.org/10.5194/acp-12-6699-2012>

395

396 Fuzzi, S., Andreae, M. O., Huebert, B. J., Kulmala, M., Bond, T. C., Boy, M., ... Pöschl, U.  
397 (2006). Critical assessment of the current state of scientific knowledge, terminology, and  
398 research needs concerning the role of organic aerosols in the atmosphere, climate, and  
399 global change. *Atmos. Chem. Phys.*, 6(7), 2017–2038. <https://doi.org/10.5194/acp-6-2017-2006>

400

401

402 Gao, M., Carmichael, G. R., Wang, Y., Ji, D., Liu, Z., & Wang, Z. (2016). Improving simulations  
403 of sulfate aerosols during winter haze over Northern China: the impacts of heterogeneous

404 oxidation by NO<sub>2</sub>. *Frontiers of Environmental Science & Engineering*, 10(5), 16.  
405 <https://doi.org/10.1007/s11783-016-0878-2>

406

407 Goldstein, A. H., Goulden, M. L., Munger, J. W., Wofsy, S. C., & Geron, C. D. (1998). Seasonal  
408 course of isoprene emissions from a midlatitude deciduous forest. *Journal of Geophysical  
409 Research: Atmospheres*, 103(D23), 31045–31056. <https://doi.org/10.1029/98JD02708>

410

411 Greaver, T. L., Sullivan, T. J., Herrick, J. D., Barber, M. C., Baron, J. S., Cosby, B. J., ... Novak,  
412 K. J. (2012). Ecological effects of nitrogen and sulfur air pollution in the US: what do we  
413 know? *Frontiers in Ecology and the Environment*, 10(7), 365–372.  
414 <https://doi.org/10.1890/110049>

415

416 Griffiths, P. T., Badger, C. L., Cox, R. A., Folkers, M., Henk, H. H., & Mentel, T. F. (2009).  
417 Reactive Uptake of N<sub>2</sub>O<sub>5</sub> by Aerosols Containing Dicarboxylic Acids. Effect of Particle  
418 Phase, Composition, and Nitrate Content. *The Journal of Physical Chemistry A*, 113(17),  
419 5082–5090. <https://doi.org/10.1021/jp8096814>

420

421 Guenther, A., Karl, T., Harley, P., Wiedinmyer, C., Palmer, P. I., & Geron, C. (2006). Estimates  
422 of global terrestrial isoprene emissions using MEGAN (Model of Emissions of Gases and  
423 Aerosols from Nature). *Atmos. Chem. Phys.*, 6(11), 3181–3210. <https://doi.org/10.5194/acp-6-3181-2006>

425

426 Heald, C. L., Collett Jr., J. L., Lee, T., Benedict, K. B., Schwandner, F. M., Li, Y., ... Pye, H. O.  
427 T. (2012). Atmospheric ammonia and particulate inorganic nitrogen over the United States.  
428 *Atmos. Chem. Phys.*, 12(21), 10295–10312. <https://doi.org/10.5194/acp-12-10295-2012>

429

430 Irwin, J. G., & Williams, M. L. (1988). Acid rain: Chemistry and transport. *Environmental  
431 Pollution*, 50(1), 29–59. [https://doi.org/https://doi.org/10.1016/0269-7491\(88\)90184-4](https://doi.org/https://doi.org/10.1016/0269-7491(88)90184-4)

432

433 Jacob, D. J., & Winner, D. A. (2009). Effect of climate change on air quality. *Atmospheric  
434 Environment*, 43(1), 51–63. <https://doi.org/https://doi.org/10.1016/j.atmosenv.2008.09.051>

435

436 Jacobson, M. C., Hansson, H.-C., Noone, K. J., & Charlson, R. J. (2000). Organic atmospheric  
437 aerosols: Review and state of the science. *Reviews of Geophysics*, 38(2), 267–294.  
438 <https://doi.org/10.1029/1998RG000045>

439

440 Jimenez, J. L., Canagaratna, M. R., Donahue, N. M., Prevot, A. S. H., Zhang, Q., Kroll, J. H., ...  
441 Worsnop, D. R. (2009). Evolution of Organic Aerosols in the Atmosphere. *Science*,  
442 326(5959), 1525 LP-1529. <https://doi.org/10.1126/science.1180353>

443

444 Kelly, T. J., Smith, D. L., & Satola, J. (1999). Emission Rates of Formaldehyde from Materials  
445 and Consumer Products Found in California Homes. *Environmental Science & Technology*,  
446 33(1), 81–88. <https://doi.org/10.1021/es980592+>

447

448 Kirchstetter, T. W., Harley, R. A., & Littlejohn, D. (1996). Measurement of Nitrous Acid in  
449 Motor Vehicle Exhaust. *Environmental Science & Technology*, 30(9), 2843–2849.  
450 <https://doi.org/10.1021/es960135y>

451

452 Kleffmann, J. (2007). Daytime Sources of Nitrous Acid (HONO) in the Atmospheric Boundary  
453 Layer. *ChemPhysChem*, 8(8), 1137–1144. <https://doi.org/10.1002/cphc.200700016>

454

455 Klonecki, A., & Levy II, H. (1997). Tropospheric chemical ozone tendencies in CO-CH<sub>4</sub>-NO<sub>y</sub>-  
456 H<sub>2</sub>O system: Their sensitivity to variations in environmental parameters and their  
457 application to a global chemistry transport model study. *Journal of Geophysical Research: Atmospheres*, 102(D17), 21221–21237. <https://doi.org/10.1029/97JD01805>

459

460 Levy II, H., Mahlman, J. D., Moxim, W. J., & Liu, S. C. (1985). Tropospheric ozone: The role of  
461 transport. *Journal of Geophysical Research: Atmospheres*, 90(D2), 3753–3772.  
462 <https://doi.org/10.1029/JD090iD02p03753>

463

464 Levy, H. (1971). Normal Atmosphere: Large Radical and Formaldehyde Concentrations  
465 Predicted. *Science*, 173(3992), 141 LP-143. <https://doi.org/10.1126/science.173.3992.141>

466

467 Li, J., Gong, C., Wang, E., Yu, X., Wang, Z., & Liu, X. (2010). Emissions of Formaldehyde and  
468 Unburned Methanol from a Spark-Ignition Methanol Engine during Cold Start. *Energy &*  
469 *Fuels*, 24(2), 863–870. <https://doi.org/10.1021/ef9009982>

470

471 Li, Q., Zhang, L., Wang, T., Tham, Y. J., Ahmadov, R., Xue, L., ... Zheng, J. (2016). Impacts of  
472 heterogeneous uptake of dinitrogen pentoxide and chlorine activation on ozone and reactive  
473 nitrogen partitioning: improvement and application of the WRF-Chem model in southern  
474 China. *Atmos. Chem. Phys.*, 16(23), 14875–14890. <https://doi.org/10.5194/acp-16-14875-2016>

475

476

477 Lowe, D., Archer-Nicholls, S., Morgan, W., Allan, J., Utembe, S., Ouyang, B., ... McFiggans, G.  
478 (2015). WRF-Chem model predictions of the regional impacts of N<sub>2</sub>O<sub>5</sub> heterogeneous  
479 processes on night-time chemistry over north-western Europe. *Atmos. Chem. Phys.*, 15(3),  
480 1385–1409. <https://doi.org/10.5194/acp-15-1385-2015>

481

482 Luecken, D. J., Hutzell, W. T., Strum, M. L., & Pouliot, G. A. (2012). Regional sources of  
483 atmospheric formaldehyde and acetaldehyde, and implications for atmospheric modeling.  
484 *Atmospheric Environment*, 47, 477–490.  
485 <https://doi.org/https://doi.org/10.1016/j.atmosenv.2011.10.005>

486

487 McDuffie, E. E., Fibiger, D. L., Dubé, W. P., Lopez Hilfiker, F., Lee, B. H., Jaeglé, L., ... Brown,  
488 S. S. (2018). ClNO<sub>2</sub> Yields From Aircraft Measurements During the 2015 WINTER  
489 Campaign and Critical Evaluation of the Current Parameterization. *Journal of Geophysical  
490 Research: Atmospheres*, 123(22), 12,15,913-994. <https://doi.org/10.1029/2018JD029358>

491

492 McDuffie, E. E., Fibiger, D. L., Dubé, W. P., Lopez-Hilfiker, F., Lee, B. H., Thornton, J. A., ...  
493 Brown, S. S. (2018). Heterogeneous N<sub>2</sub>O<sub>5</sub> Uptake During Winter: Aircraft Measurements  
494 During the 2015 WINTER Campaign and Critical Evaluation of Current Parameterizations.  
495 *Journal of Geophysical Research: Atmospheres*, 123(8), 4345–4372.  
496 <https://doi.org/10.1002/2018JD028336>

497

498 Menz, F. C., & Seip, H. M. (2004). Acid rain in Europe and the United States: an update.  
499 *Environmental Science & Policy*, 7(4), 253–265.  
500 <https://doi.org/https://doi.org/10.1016/j.envsci.2004.05.005>

501

502 Orlando, J. J., Tyndall, G. S., Apel, E. C., Riemer, D. D., & Paulson, S. E. (2003). Rate  
503 coefficients and mechanisms of the reaction of Cl-atoms with a series of unsaturated  
504 hydrocarbons under atmospheric conditions. *International Journal of Chemical Kinetics*,  
505 35(8), 334–353. <https://doi.org/10.1002/kin.10135>

506  
507 Peirce, T., Geron, C., Bender, L., Dennis, R., Tonnesen, G., & Guenther, A. (1998). Influence of  
508 increased isoprene emissions on regional ozone modeling. *Journal of Geophysical*  
509 *Research: Atmospheres*, 103(D19), 25611–25629. <https://doi.org/10.1029/98JD01804>

510  
511 Platt, U., & Hönniger, G. (2003). The role of halogen species in the troposphere. *Chemosphere*,  
512 52(2), 325–338. [https://doi.org/10.1016/S0045-6535\(03\)00216-9](https://doi.org/10.1016/S0045-6535(03)00216-9)

513  
514 Platt, U. F., Winer, A. M., Biermann, H. W., Atkinson, R., & Pitts, J. N. (1984). Measurement of  
515 nitrate radical concentrations in continental air. *Environmental Science & Technology*,  
516 18(5), 365–369. <https://doi.org/10.1021/es00123a015>

517  
518 Platt, U., & Heintz, F. (1994). Nitrate Radicals in Tropospheric Chemistry. *Israel Journal of*  
519 *Chemistry*, 34(3-4), 289–300. <https://doi.org/10.1002/ijch.199400033>

520  
521 Ramanathan, V., & Feng, Y. (2009). Air pollution, greenhouse gases and climate change: Global  
522 and regional perspectives. *Atmospheric Environment*, 43(1), 37–50.  
523 <https://doi.org/10.1016/j.atmosenv.2008.09.063>

524  
525 Richards, L. W. (1983). Comments on the oxidation of NO<sub>2</sub> to nitrate—day and night.  
526 *Atmospheric Environment* (1967), 17(2), 397–402.  
527 [https://doi.org/10.1016/0004-6981\(83\)90057-4](https://doi.org/10.1016/0004-6981(83)90057-4)

528  
529 Riedel, T. P., Wolfe, G. M., Danas, K. T., Gilman, J. B., Kuster, W. C., Bon, D. M., ... Thornton,  
530 J. a. (2014). An MCM modeling study of nitryl chloride (ClNO<sub>2</sub>) impacts on oxidation,  
531 ozone production and nitrogen oxide partitioning in polluted continental outflow.  
532 *Atmospheric Chemistry and Physics*, 14(8), 3789–3800. <https://doi.org/10.5194/acp-14-3789-2014>

533  
534 Roberts, J. M. (1990). The atmospheric chemistry of organic nitrates. *Atmospheric Environment*.  
535 *Part A. General Topics*, 24(2), 243–287. [https://doi.org/10.1016/0960-1686\(90\)90108-Y](https://doi.org/10.1016/0960-1686(90)90108-Y)

536  
537 Roberts, J. M., Osthoff, H. D., Brown, S. S., Ravishankara, A. R., Coffman, D., Quinn, P., &  
538 Bates, T. (2009). Laboratory studies of products of N<sub>2</sub>O<sub>5</sub> uptake on Cl<sup>−</sup> containing  
539 substrates. *Geophysical Research Letters*, 36(20). <https://doi.org/10.1029/2009GL040448>

540  
541 Ryder, O. S., Campbell, N. R., Shaloski, M., Al-Mashat, H., Nathanson, G. M., & Bertram, T. H.  
542 (2015). Role of Organics in Regulating ClNO<sub>2</sub> Production at the Air–Sea Interface. *The*  
543 *Journal of Physical Chemistry A*, 119(31), 8519–8526. <https://doi.org/10.1021/jp5129673>

544  
545 Sarwar, G., Simon, H., Xing, J., & Mathur, R. (2014). Importance of tropospheric ClNO<sub>2</sub>  
546 chemistry across the Northern Hemisphere. *Geophysical Research Letters*, 41(11), 4050–  
547 4058. <https://doi.org/10.1002/2014GL059962>

548  
549 Schofield, C. L. (1976). Acid Precipitation: Effects on Fish. *Ambio*, 5(5/6), 228–230. Retrieved  
550 from <http://www.jstor.org/stable/4312222>

551  
552 Seinfeld, J. H. (1989). Urban Air Pollution: State of the Science. *Science*, 243(4892), 745–752.  
553 <https://doi.org/10.1126/science.243.4892.745>

554  
555  
556

557 Shepson, P. B., Hastie, D. R., So, K. W., Schiff, H. I., & Wong, P. (1992). Relationships between  
558 PAN, PPN and O<sub>3</sub> at urban and rural sites in Ontario. *Atmospheric Environment. Part A. General Topics*, 26(7), 1259–1270. [https://doi.org/https://doi.org/10.1016/0960-1686\(92\)90387-Z](https://doi.org/https://doi.org/10.1016/0960-1686(92)90387-Z)

561

562 Sigsby, J. E., Tejada, S., Ray, W., Lang, J. M., & Duncan, J. W. (1987). Volatile organic  
563 compound emissions from 46 in-use passenger cars. *Environmental Science & Technology*, 21(5), 466–475. <https://doi.org/10.1021/es00159a007>

564

565 Singh, H. B., & Hanst, P. L. (1981). Peroxyacetyl nitrate (PAN) in the unpolluted atmosphere: An  
566 important reservoir for nitrogen oxides. *Geophysical Research Letters*, 8(8), 941–944.  
<https://doi.org/10.1029/GL008i008p00941>

567

568 Smith, N., Plane, J. M. C., Nien, C.-F., & Solomon, P. A. (1995). Nighttime radical chemistry in  
569 the San Joaquin Valley. *Atmospheric Environment*, 29(21), 2887–2897.  
[https://doi.org/https://doi.org/10.1016/1352-2310\(95\)00032-T](https://doi.org/https://doi.org/10.1016/1352-2310(95)00032-T)

570

571

572

573 Stutz, J., Alicke, B., Ackermann, R., Geyer, A., White, A., & Williams, E. (2004). Vertical  
574 profiles of NO<sub>3</sub>, N<sub>2</sub>O<sub>5</sub>, O<sub>3</sub>, and NO<sub>x</sub> in the nocturnal boundary layer: 1. Observations  
575 during the Texas Air Quality Study 2000. *Journal of Geophysical Research: Atmospheres*,  
576 109(D12). <https://doi.org/10.1029/2003JD004209>

577

578

579 Stutz, J., Alicke, B., & Neftel, A. (2002). Nitrous acid formation in the urban atmosphere:  
580 Gradient measurements of NO<sub>2</sub> and HONO over grass in Milan, Italy. *Journal of  
581 Geophysical Research: Atmospheres*, 107(D22), LOP 5-1-LOP 5-15.  
<https://doi.org/10.1029/2001JD000390>

582

583

584 Tesche, T. W., Morris, R., Tonnesen, G., McNally, D., Boylan, J., & Brewer, P. (2006).  
585 CMAQ/CAMx annual 2002 performance evaluation over the eastern US. *Atmospheric  
586 Environment*, 40(26), 4906–4919.  
<https://doi.org/https://doi.org/10.1016/j.atmosenv.2005.08.046>

587

588

589 Vinken, G. C. M., Boersma, K. F., Jacob, D. J., & Meijer, E. W. (2011). Accounting for non-  
590 linear chemistry of ship plumes in the GEOS-Chem global chemistry transport model.  
591 *Atmos. Chem. Phys.*, 11(22), 11707–11722. <https://doi.org/10.5194/acp-11-11707-2011>

592

593 Volkamer, R., Jimenez, J. L., San Martini, F., Dzepina, K., Zhang, Q., Salcedo, D., ... Molina, M.  
594 J. (2006). Secondary organic aerosol formation from anthropogenic air pollution: Rapid and  
595 higher than expected. *Geophysical Research Letters*, 33(17).  
<https://doi.org/10.1029/2006GL026899>

596

597

598 Walker, J. M., Philip, S., Martin, R. V., & Seinfeld, J. H. (2012). Simulation of nitrate, sulfate,  
599 and ammonium aerosols over the United States. *Atmos. Chem. Phys.*, 12(22), 11213–11227.  
<https://doi.org/10.5194/acp-12-11213-2012>

600

601

602 Wang, W. C., Yung, Y. L., Lacis, A. A., Mo, T., & Hansen, J. E. (1976). Greenhouse Effects due  
603 to Man-Made Perturbations of Trace Gases. *Science*, 194(4266), 685 LP-690.  
<https://doi.org/10.1126/science.194.4266.685>

604

605

606 Weinstock, B. (1969). Carbon Monoxide: Residence Time in the Atmosphere. *Science*,  
607 166(3902), 224 LP-225. <https://doi.org/10.1126/science.166.3902.224>

608  
609 Wert, B. P., Trainer, M., Fried, A., Ryerson, T. B., Henry, B., Potter, W., ... Wisthaler, A. (2003).  
610 Signatures of terminal alkene oxidation in airborne formaldehyde measurements during  
611 TexAQS 2000. *Journal of Geophysical Research: Atmospheres*, 108(D3).  
612 <https://doi.org/10.1029/2002JD002502>

613  
614 Wolfe, G. M., Kaiser, J., Hanisco, T. F., Keutsch, F. N., de Gouw, J. A., Gilman, J. B., ...  
615 Warneke, C. (2016). Formaldehyde production from isoprene oxidation  
616 across NO<sub>x</sub> regimes. *Atmos. Chem. Phys.*, 16(4), 2597–2610. <https://doi.org/10.5194/acp-16-2597-2016>

617  
618 Wolfe, G. M., Marvin, M. R., Roberts, S. J., Travis, K. R., & Liao, J. (2016). The Framework for  
619 0-D Atmospheric Modeling (F0AM) v3.1. *Geosci. Model Dev.*, 9(9), 3309–3319.  
620 <https://doi.org/10.5194/gmd-9-3309-2016>

621  
622 Wong, K. W., Tsai, C., Lefer, B., Haman, C., Grossberg, N., Brune, W. H., ... Stutz, J. (2012).  
623 Daytime HONO vertical gradients during SHARP 2009 in Houston, TX. *Atmos. Chem.*  
624 *Phys.*, 12(2), 635–652. <https://doi.org/10.5194/acp-12-635-2012>

625  
626 Ye, C., Zhou, X., Pu, D., Stutz, J., Festa, J., Spolaor, M., ... Knote, C. (2016). Rapid cycling of  
627 reactive nitrogen in the marine boundary layer. *Nature*, 532, 489. Retrieved from  
628 <https://doi.org/10.1038/nature17195>

629  
630 Yienger, J. J. (1999). Correction to “An evaluation of chemistry’s role in the winter-spring ozone  
631 maximum found in the northern midlatitude free troposphere” by J. J. Yienger et al. *Journal*  
632 *of Geophysical Research*, 104(D7), 8329.

633  
634 Zetzsch, C., & Behnke, W. (1992). Heterogeneous Photochemical Sources of Atomic Cl in the  
635 Troposphere. *Berichte Der Bunsengesellschaft Für Physikalische Chemie*, 96(3), 488–493.  
636 <https://doi.org/10.1002/bbpc.19920960351>

637  
638 Zhou, X., Zhang, N., TerAvest, M., Tang, D., Hou, J., Bertman, S., ... Stevens, P. S. (2011).  
639 Nitric acid photolysis on forest canopy surface as a source for tropospheric nitrous acid.  
640 *Nature Geoscience*, 4, 440. Retrieved from <https://doi.org/10.1038/ngeo1164>

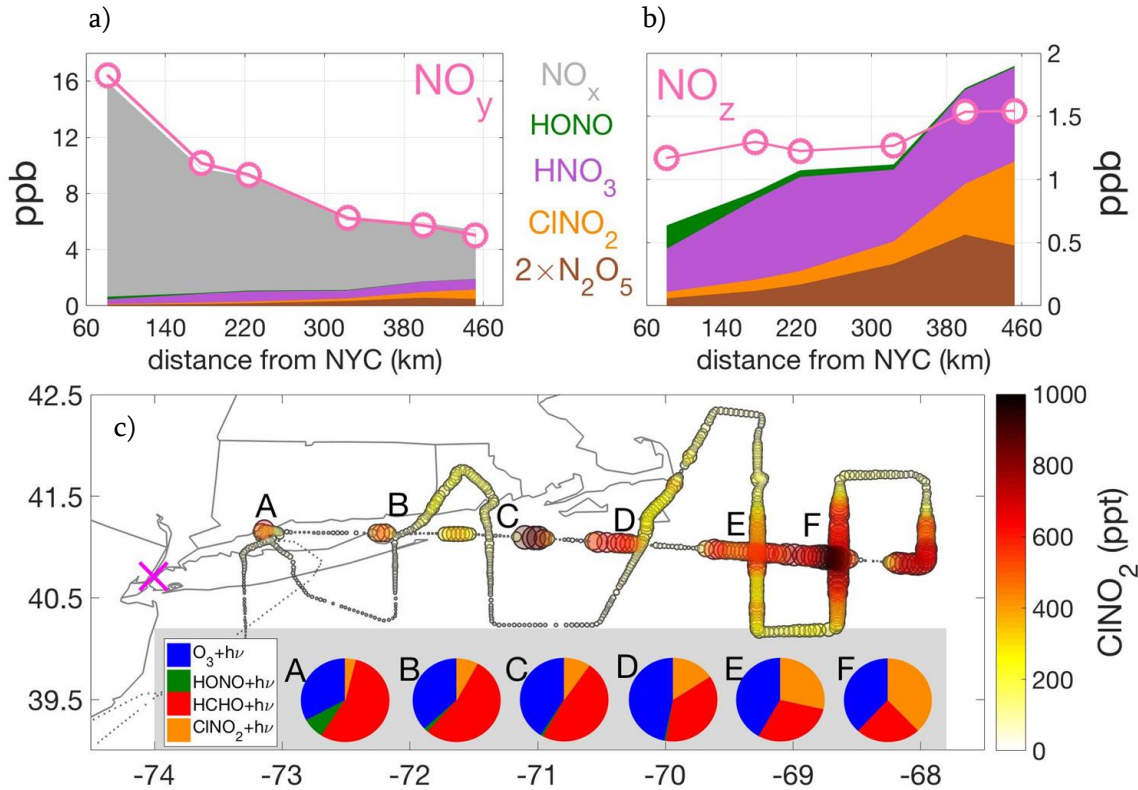


**Figure 1. Top panels:** evolution of nitrogen oxide reservoirs downwind of New York City observed aboard the NSF/NCAR C-130 aircraft during Research Flight 3 (RF; February 7, 2015) of the WINTER campaign. Observations are from below 2 km altitude only, and correspond to 7pm to 11pm local time.  $\text{NO}_y$  represents the sum of all forms of oxidized nitrogen that can be converted to  $\text{NO}$  at high temperatures (a)  $\text{NO}_z$  represents the sum of all oxidized nitrogen species except for  $\text{NO}_x$  ( $\text{NO} + \text{NO}_2$ ) and is derived from the measured  $\text{NO}_y - \text{NO}_x$  (b). The gap between total  $\text{NO}_z$  and the sum of individual components that occurs near to NYC, while within the total calibration uncertainty of the sum, can likely be explained by a combination of  $\text{pNO}_3^-$  and peroxy nitrates (see SI). (c) map of the flight track colored and sized by the measured mixing ratio of  $\text{CINO}_2$ . The nearly straight trajectory between points A through F consisted of periodic ascents and descents of the aircraft between 500 and 2000 m altitude, profiling the vertical extent of the polluted atmospheric boundary layer. Pie charts show the observationally constrained contributions of different radical precursors to the integrated daytime radical source (see text).

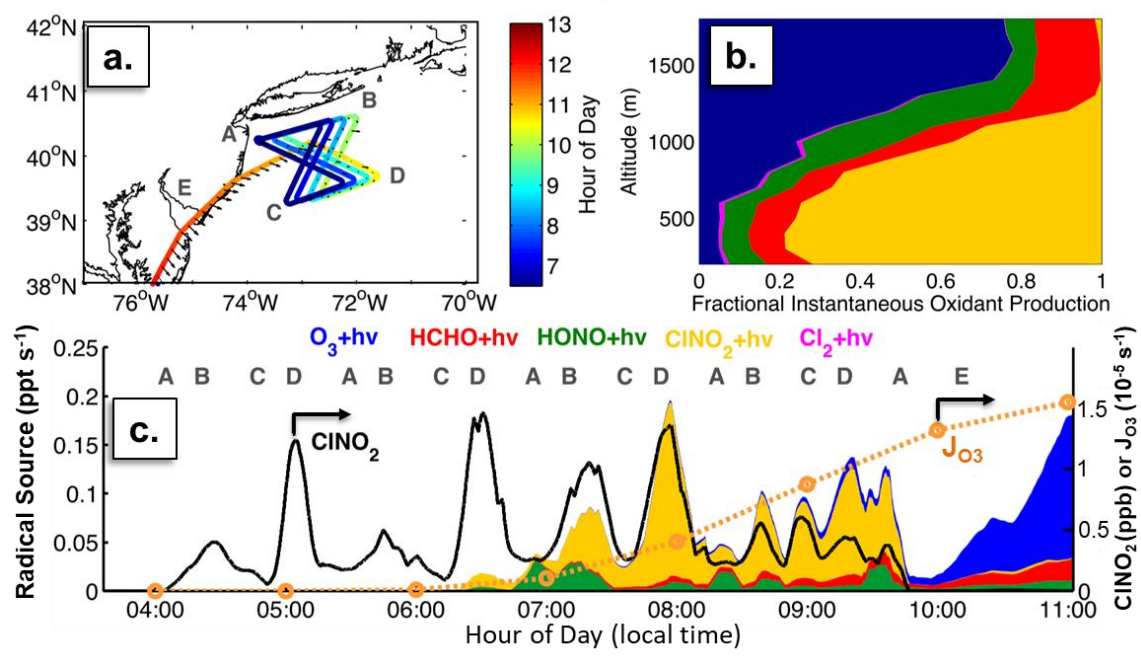
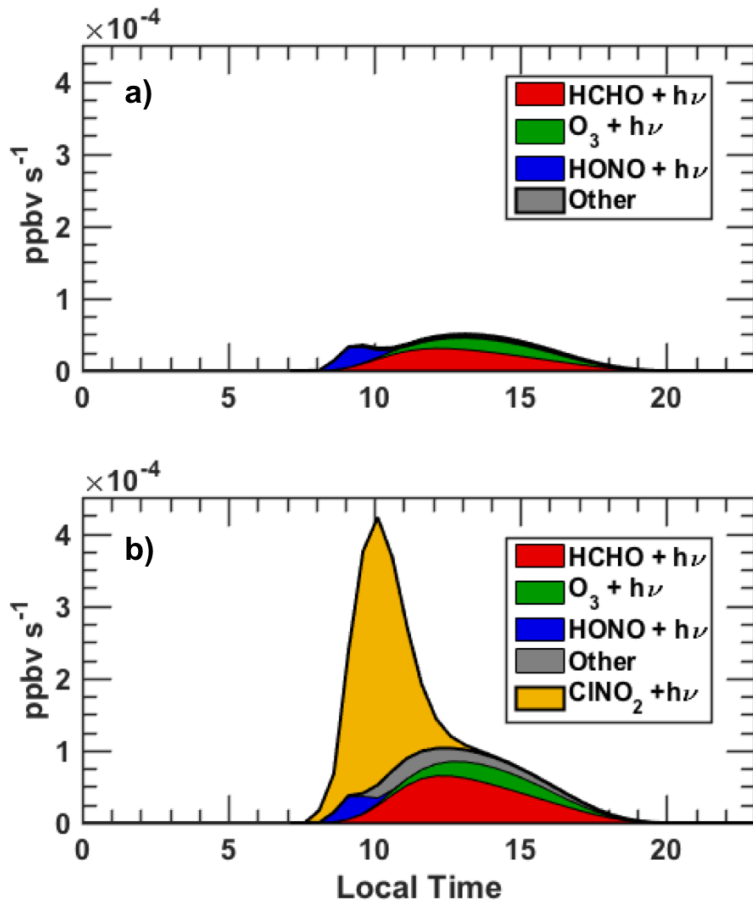
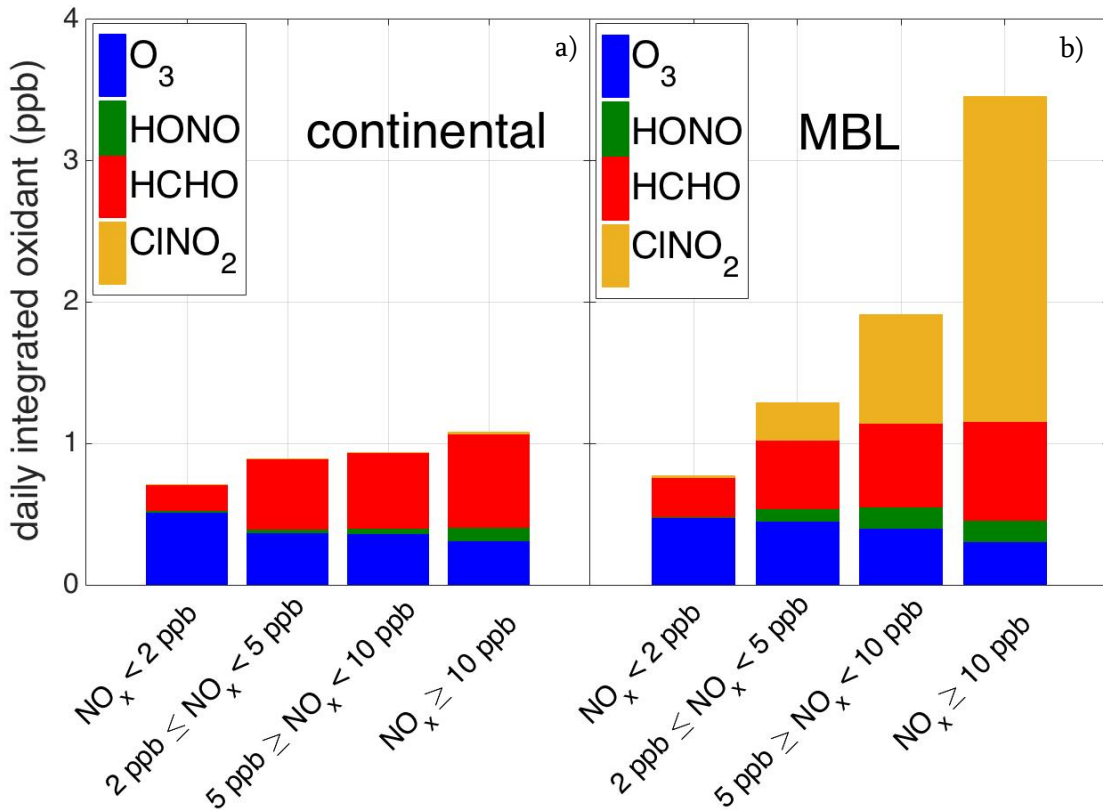


Figure 2. (a) Flight track of the NSF/NCAR C-130 on Research Flight 8 of the WINTER campaign, colored by local time of day. Sunrise occurred at approximately 6:30 AM local time. Only portions with altitudes <2000 m are shown. (b) Vertical profiles of the instantaneous radical source calculated from observations of solar radiation and radical precursors. (c) Time series of the instantaneous radical source (left axis, stacked color),  $\text{CINO}_2$  mixing ratios (right axis, ppb), and the  $\text{O}_3$  photolysis frequency (orange circles, right axis,  $10^{-5} \text{ s}^{-1}$ )



**Figure 3.** Summary of daily, net primary radical production rates calculated the day following our interception of the peak  $\text{CINO}_2$  concentrations on RF08 using the FOAM box model initialized with WINTER observations without including chlorine reactions (a) and including chlorine reactions (b).



**Figure 4.** Summary of daily primary radical source calculated from observations of  $O_3$ ,  $H_2O$ ,  $CINO_2$ ,  $HONO$ , and  $HCHO$  made during the daytime in the continental boundary layer (a), and at night within the MBL (b). Data are binned as a function of observed  $NO_x$  mixing ratios with lower values indicating less polluted air and higher values indicating more polluted air. In the left pane, we show only daytime observations over land, as these better reflect a well-mixed polluted boundary layer. For comparison, we show estimates based on nighttime observations within the MBL in the right panel. These two regimes are a fair representation of the typical importance of each radical source over the entire data set. See SI for additional statistics and calculations).

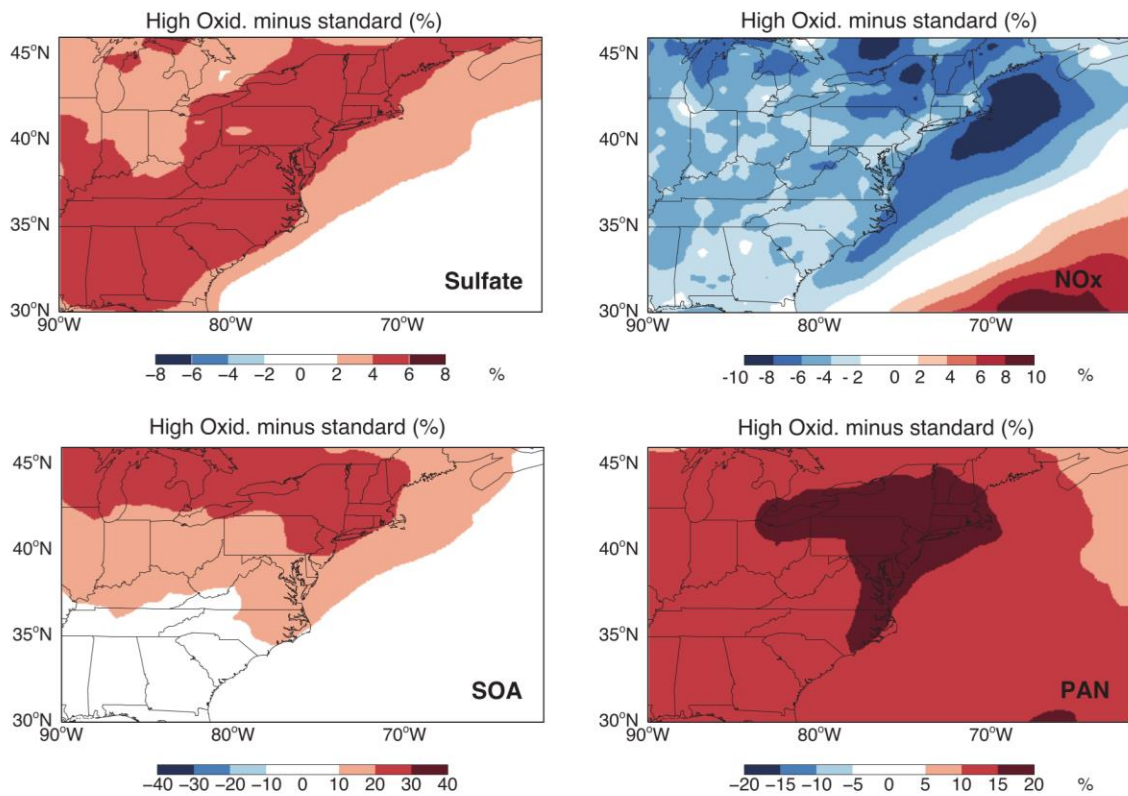


**Figure 5.** Relative changes in GEOS-Chem model predicted sulfate, SOA, NO<sub>x</sub> and PAN abundances between runs using standard emissions and chemistry, and those using updated emissions of HCHO and ClNO<sub>2</sub> chemistry based on the WINTER observations. Enhanced oxidative capacity in the boundary layer from enhanced HCHO (over land) and ClNO<sub>2</sub> (in the MBL) leads to increased conversion of SO<sub>2</sub> to sulfate aerosol mass, VOC to secondary organic aerosol mass, and increased conversion of NO<sub>x</sub> into reservoirs such as PAN which in turn affects its global distribution.

721  
722